Mon. Not. R. Astron. Soc. **348,** 1379–1387 (2004) doi:10.1111/j.1365-2966.2004.07467.x

Radio–optical flux behaviour and spectral energy distribution of the intermediate blazar GC 0109+224

Stefano Ciprini,[1,2⋆] Gino Tosti,[1,2] Harri Teräsranta[3] and Hugh D. Aller[4]

[1] *Physics Department and Astronomical Observatory, University of Perugia, via Pascoli, 06123 Perugia, Italy*
[2] *INFN, Perugia Section, via Pascoli, 06123 Perugia, Italy*
[3] *Metsähovi Radio Observatory, Helsinki University of Technology, 02540 Kylmälä, Finland*
[4] *Department of Astronomy, Dennison Bldg, University of Michigan, Ann Arbor, MI 48109, USA*

Accepted 2003 November 22. Received 2003 September 22; in original form 2003 June 20

ABSTRACT

About 20 years of radio observations of the BL Lac object GC 0109+224 (S2 0109+22, RGB J0112+227) in five bands (from 4.8 to 37 GHz) are presented and analysed together with optical data. Over the past 10 years this blazar has exhibited enhanced activity. There is only weak correlation between radio and optical flare delays, usually protracted on longer time-scales in the radio with respect to the optical. In some cases no radio flare counterpart was observed for the optical outbursts. The radio variability, characterized by peak superposition, shows hints of some characteristic time-scales (around the 3–4 yr), and a fluctuation mode between the flickering and the shot noise. The reconstructed spectral energy distribution, poorly monitored at high energies, is preliminarily parametrized with a synchrotron–self-Compton description. The smooth synchrotron continuum, peaked in the near-infrared–optical bands, strengthens the hypothesis that this source could be an intermediate blazar. Moreover, the intense flux in millimetre bands, and the optical and X-ray brightness, might suggest a possible detectable γ-ray emission.

Key words: radiation mechanisms: non-thermal – methods: statistical – BL Lacertae objects: general – BL Lacertae objects: individual: 0109+224 – BL Lacertae objects: individual: 0112+227 – radio continuum: galaxies.

1 INTRODUCTION

The compact radio-loud source GC 0109+224 (S2 0109+22, TXS 0109+224, RX J0112.0+2244, EF B0109+2228, RGB J0112+227), belonging to the Green Bank radio survey list C, is a synchrotron source discovered more than 30 years ago (Pauliny-Toth et al. 1972) and optically identified a few years later (Owen & Mufson 1977). It is a strong radio–millimetre active galactic nucleus (AGN), with variable flux, polarization degree and position angle, showing a flat average spectrum much like the classical BL Lac objects. Unfortunately it is poorly studied beyond optical frequencies. The milliarcsecond (parsec) scale of GC 0109+224 reveals a compact core, and a secondary component with no additional diffuse emission, and less luminous and/or beamed than the 1-Jy sample sources (Fey & Charlot 2000; Bondi et al. 2001). The kiloparsec scale shows a faint one-sided collimated radio jet, about 2 arcsec long (Wilkinson et al. 1998), largely misaligned with the parsec-scale inner region, as is frequently observed in high-luminosity and low-energy peaked BL Lac objects (LBLs, with the peak in the infrared bands). This source is a member of the 200-mJy catalogue (Marchã et al. 1996), a sample that seems to fill the gap between the high-energy peaked BL Lacs (HBLs, with the peak in the ultraviolet or soft X-ray bands) and the LBLs, as expected by some current blazar unification pictures.

The historical optical light curve shows a behaviour intermediate between the larger-amplitude variable BL Lacs and the smaller-amplitude variable flat-spectrum radio quasar (FSRQs). Increased flare activity (rapid optical variations, peak superposition, rapid flux drops) is clearly shown after 1994 in the optical bands, as a result of the increased data sampling of the Perugia University Observatory, which has also recorded the larger and faster flares (Ciprini et al. 2003a). In the course of seven years, GC 0109+224 showed six main optical outbursts (weeks/month scale), and a variability mode placed between the flickering and the shot noise.

Rather achromatic long-term optical behaviour is accompanied by isolated outbursts with loop-like hysteresis of the spectral index, indicating that rapid optical variability is dominated by non-thermal cooling of a single electron population (Ciprini et al. 2003a). Both the optical flux and the polarization are known to be variable on different time-scales, including intra-day variability (Sitko, Schmidt & Stein 1985; Mead et al. 1990; Valtaoja et al. 1991). The relatively strong variable degree (up to 30 per cent) and direction of the optical linear polarization is one of the most noticeable characteristics

⋆E-mail: stefano.ciprini@pg.infn.it

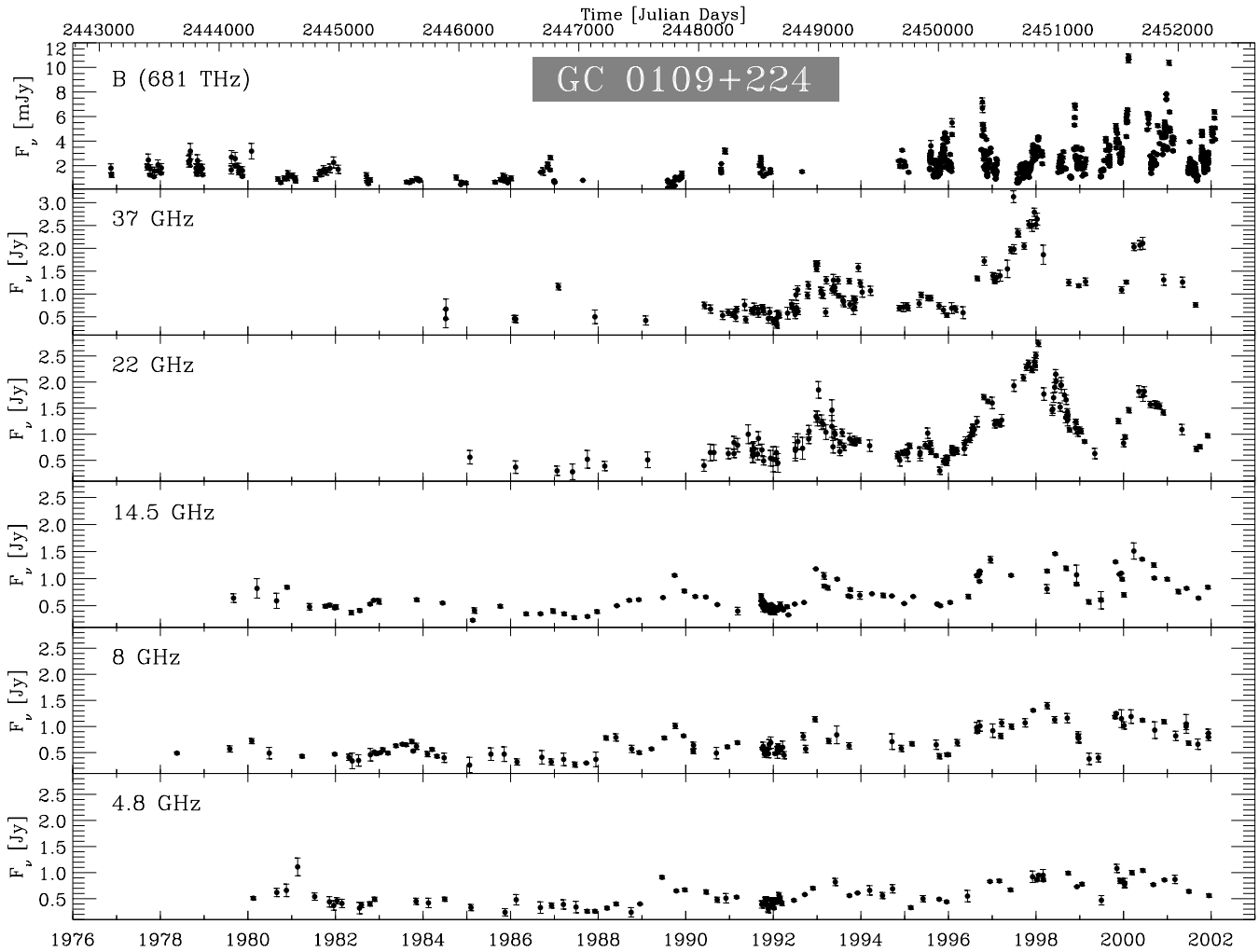

Figure 1. The complete radio–optical density flux light curves of GC 0109+224. The optical observations are historical and the Perugia Observatory (Italy) data (post-1994 data points), reported in the original or extrapolated Johnson *B* band (see for details Ciprini et al. 2003a). The high sampled data at 37 and 22 GHz are from Metsähovi (Finland), and the 14.5, 8 and 4.8 GHz data are from the long-term monitoring of the UMRAO (USA). This source clearly exhibits a higher mean flux level, and an enhanced activity in the radio–millimetre after 1992, and in the optical after 1994, even if the optical sampling before this year is insufficient to record faster (and usually larger) flares.

of this object (Takalo 1991; Valtaoja et al. 1993), even if there is no clear correlation between the flux level and polarization degree. The host galaxy of GC 0109+224 is still unresolved (Falomo 1996; Wright et al. 1998), but a lower limit to the redshift $z \geqslant 0.4$ is suggested (Falomo 1996). From the old *IRAS* data, there is no evidence for a thermal component in the far-infrared (Impey & Neugebauer 1988).

GC 0109+224 was detected in the past at X-ray bands by the *Einstein*, *EXOSAT* and *ROSAT* satellites, and the source is a member of the RGB catalogue (Laurent-Muehleisen et al. 1999), a list of intermediate blazars with properties smoothly distributed in a large range between the LBL and HBL subclasses. In the diagnostic diagram $\alpha_{\rm ro}$–$\alpha_{\rm oX}$ (Padovani & Giommi 1995), GC 0109+224 appears close (Dennett-Thorpe & Marchã 2000) to a prototype of intermediate blazars like ON 231 (W Com, Tagliaferri et al. 2000; Tosti et al. 2002; Böttcher, Mukherjee & Reimer 2002). The HBL and LBL subclasses exhibit systematically distinct properties (i.e. $F_{\rm X}/F_{\rm rad}$ flux density ratio, degree of radio core dominance, optical polarization degree and variability, etc.). The so-called 'intermediate' blazars are critical to clarify the relationship between these subclasses, and to validate the unified schemes based on bolometric power. Intermediate blazars often peak in optical bands (thus are selected and monitored mainly by optical telescopes), and during some variability phases the break between the two overall spectral components occurs in the X-ray bands. In some cases their spectral energy distributions (SEDs) can still be well described with synchrotron–self-Compton (SSC) models (like for the HBLs), and this implies, by simple scaling arguments, a possible inverse Compton (IC) emission peaked in GeV γ-ray bands (see e.g. Stecker, de Jager & Salamon 1996). In the case of GC 0109+224, EGRET did not detect any γ-ray emission (phase 1, Fichtel et al. 1994), with a rather low upper limit of 0.01 nJy above 100 MeV.

GC 0109+224 is regularly monitored by the University of Michigan Radio Astronomy Observatory (UMRAO) (see e.g. Aller, Aller & Hughes 1996) and by the Metsähovi Radio Observatory, Finland (see e.g. Teräsranta et al. 1998). In order to search for time correlations between the optical and radio fluctuations at the various bands, in Section 2 the updated radio flux data of UMRAO and Metsähovi are compared with the available optical data (reported in Ciprini et al. 2003a). In Section 3 the temporal behaviour of the radio light curves is investigated through well-known methods suitable for unevenly sampled data sets. In Section 4 we show the reconstruction

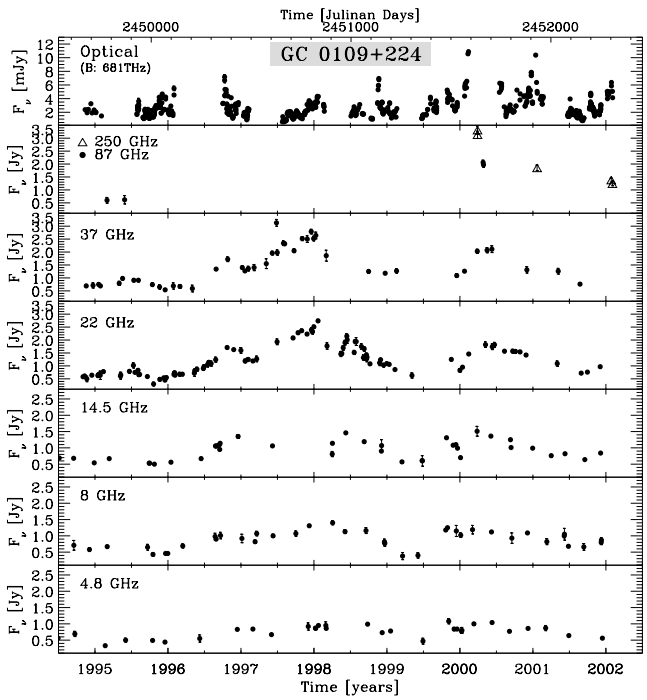

Figure 2. The post-1994 portion of the flux curves in Fig. 1, which match the optically best-sampled period. A few observations at millimetre wavelength (87 and 250 GHz) are also added in this plot. In this detail radio flares clearly appear to work on considerably longer time-scales, with respect to the optical flares. The relevant emission bump between the end of 1995 and mid-1999 (clearly visible in the 22-GHz curve) seems to be the result of superposition of either four flares departing from base level, or of four peaks departing from a slower base level bump. Noteworthy is also the 2000 February–April outburst, because it seems to be detected (during the last decreasing phase) at all seven millimetre–radio frequencies reported in this plot.

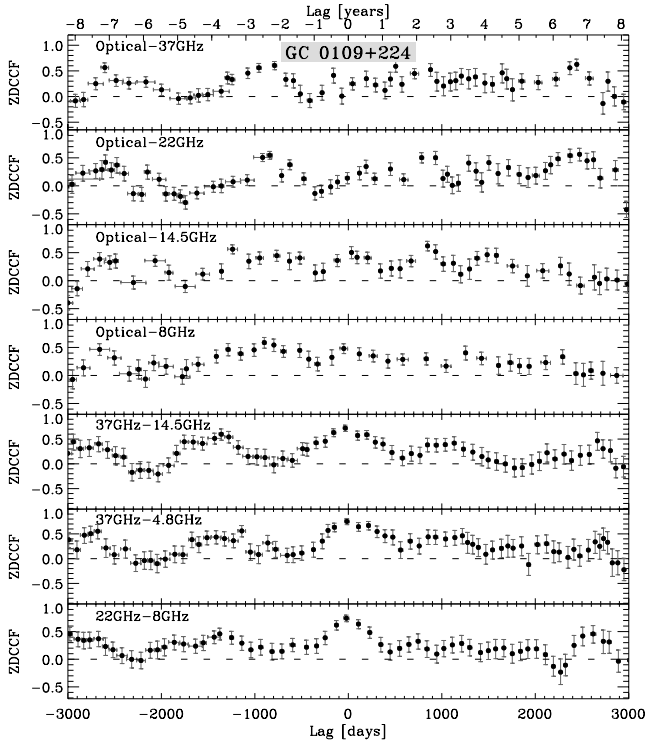

Figure 3. Cross-correlation calculated with the z-transformed discrete correlation function (ZDCF, Alexander 1997). Owing to the different time-scales for the duty cycles in the radio and optical, and to gaps empty of data in the optical, no strong evidence of a radio–optical correlation is found. Weak peaks in the cross-correlations (ZDCCF coefficient $\simeq$ 0.5–0.6) are found around a lag of 900 d (also positive in the optical–22 GHz correlations, see text). On the other hand, the fluxes at the various radio frequencies appear well correlated, as expected, with a peak around the zero lag.

of the SED, with the available multiwavelength data, and a first estimation of the bolometric energy and physical parameters using a pure SSC model.

2 RADIO–OPTICAL CORRELATIONS

The reconstructed optical flux history of GC 0109+224 and the last seven years of data mainly collected during the Perugia monitoring programme are compared with the updated radio flux observations from the Metsähovi (37 and 22 GHz data) and UMRAO (14.5, 8 and 4.8 GHz data) radio observatories. At centimetre and millimetre bands (up to about 90 GHz), a monthly sampling for blazars is enough in most cases. The source was monitored at an appreciable rate, especially at 22 GHz, and for a significant long-term period at 4.8, 8 and 14.5 GHz. Some essential properties of the centimetre emission of this blazar measured at UMRAO are outlined in (Aller et al. 1999). Metsähovi data up to 1998 were compared with a few literature optical observations (only 1996–1998), finding a lag of about 400 d between optical and 22-GHz variations (Hanski, Takalo & Valtaoja 2002).

The complete optical (Johnson B band) and radio light curves of GC 0109+224 are plotted in Fig. 1. Increased activity was observed after 1992 in all five radio bands. Prior to 1995, available optical data are too few to check the beginning of enhanced emission at this band. Since 1995, Perugia observations have increased the sampling density, recording also the larger (and faster) flares, showing increased activity, rapid variations and the same flare superposition that seems to characterize the radio flux. The flux history of the source, with millimetre data added, is plotted in Fig. 2 in more detail. Radio outbursts are clearly longer than the optical one, and show smaller amplitudes at lower frequencies. The peak frequency, in which the highest flux is observed during the flare, seems, at least for the outburst of 2000 March–April (2000.4, Fig. 2), to be around millimetre wavelengths [as an intense flux of 3.13 ± 0.04 and 3.31 ± 0.06 Jy at 250 GHz was detected by the Mambo bolometer at IRAM on 2000 March 29 (Bertoldi, private communication)].

The 22 and 37 GHz curves of Fig. 2 show the faster features in the radio, and five main peaks: around 1996.7 (visible also at 14.5, 8 and 4.8 GHz), around 1997.5, around 1998.0 (seen also at 8 GHz), still one before 1998.5 (seen also at 14.5 GHz, while the 37-GHz receiver was down), and another around 2000.4 (this is seen in all the bands). Other peaks are easily identifiable (Fig. 1) around 1993.0 (from 8 to 37 GHz), and at the end of 1989 (from 4.8 to 14.5 GHz). The more violent optical activity in these years (Fig. 2) is characterized by six main flares of much shorter duration (on the order of weeks to one month), with faster rise and decline.

The noticeable temporal structure in the radio flux curves between the end of 1995 and mid-1999 looks like an underlying emission bump spreading over 3.5 yr, with four superposed main peaks, or a superposition of four flares departing from the base level. It is difficult, even visually, to link this radio bump to a specific optical peak. The optical emission in this period, apart for an outburst in 1996 October, decreases to a base level, with a few flickering low peaks until mid-1997, then rises almost monotonically with a flickering

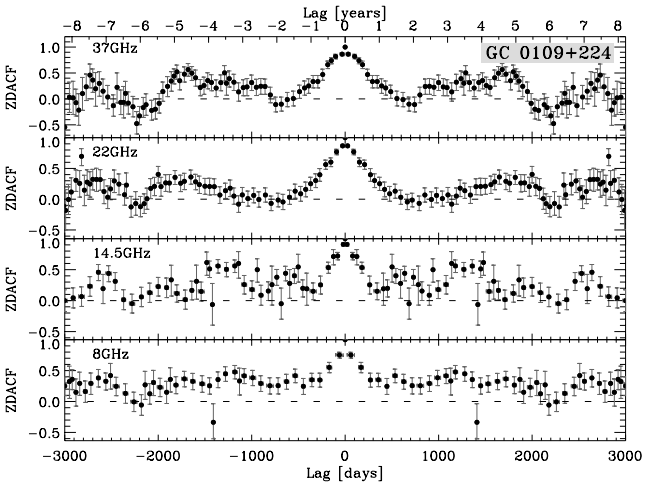

Figure 4. The autocorrelations of the radio flux curves, calculated with the ZDCF. These do not show any relevant feature, except for broad and weak (ZDACF $\simeq 0.6$) peaks around the time-scale of 3.14–4.06 yr (at 14.5 GHz), and around 3.53–4.60 yr (at 37 GHz). From 37 to 14.5 GHz, the ZDACF profile resembles shot noise, with a single bump in the correlation curve within the 2000 d time-scale (semi-amplitude $\simeq 2.7$ yr).

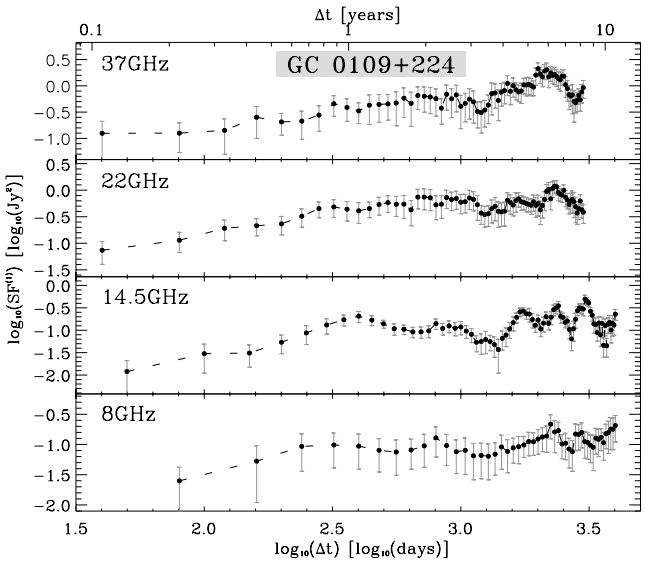

Figure 5. The first-order structure functions (SF) of the radio density flux light curves, in logarithmic scale. For the 37-GHz flux curve, the mean slope index of the steep part of the SF is $\beta = 0.48 \pm 0.08$, and for the 22-GHz curve $\beta = 0.65 \pm 0.05$ (bin size used is 40 d for both). For the 14.5-GHz series, the SF mean slope is $\beta = 0.39 \pm 0.14$, and for the 8-GHz data, $\beta = 0.52 \pm 0.13$ (50 d bin size used). The time-scales corresponding to deepest drops in the SF are 3.4–3.8 and 7.4–7.6 yr. The shorter lags at which there are hints of a flattening in the curves are around 1.1–1.8 yr.

behaviour, up to the beginning of 1998, and then displays another relevant flare only during 1998 November (Ciprini et al. 2003a). Another prominent radio outburst occurred in 2000 February–April, and seems to have been detected at all seven millimetre–radio frequencies (from 4.8 to 250 GHz, Fig. 2), during the final slow decreasing phase.

Blazars usually exhibit shorter variability time-scales, and more numerous flares in the optical, than in millimetre–radio bands, and the optical data are often heavily affected by empty gaps in the observations (seasonal interruptions and weather conditions). This is a problem in the search for correlations. The level of correlation can be investigated with the discrete correlation function (DCF, Edelson & Krolik 1988; Hufnagel & Bregman 1992), and the interpolated correlation function (ICF, Gaskell & Peterson 1987), suitable for discrete unevenly sampled data sets. In the DCF the number of points per time bin can vary greatly; in the ICF, on the other hand, the interpolation may be unreliable if the curves are undersampled. We applied a method that is more robust especially when the data are few, ensuring that there is a statistically meaningful number of points in each bin: the Fisher z-transformed DCF (ZDCF, Alexander 1997). This method builds data bins by equal population rather than equal width, and uses Monte Carlo estimations for peaks and uncertainties.

For a lag between 789 and 879 d (2.1–2.4 yr), no peaks with large values were found in the optical–radio cross-correlation curves (ZDCCF values from 0.50 to 0.62, Fig. 3). Other shorter radio–optical delays for which ZDCCF peaks are recognizable are around the delay of 190 d (observed in both the correlations with the 37 and 22 GHz fluxes, but not meaningful because ZDCCF $\simeq 0.35$), around a lag of 33 d (ZDCCF $\simeq 0.50$) between optical and 14.5-GHz curves, and around a lag of about 500 d (ZDCCF $\simeq 0.59$) between optical and 37-GHz fluxes. Interesting to note is that the cross-correlations, with a peak around the 2.1–2.4 yr lag range (both positives, delays, and negatives, leads), are found in all the optical–radio (37, 22, 14.5 and 8 GHz) correlation curves (Fig. 3). This also appears when applying the standard DCF method. Hints of optical–radio correlation around this lag time-scale are also present in the plots of (Hanski, Takalo & Valtaoja 2002), while the 350 and 400 d lags cited in this work (based only on two years of optical data) were not confirmed by our data.

Even though the coefficients are not low (0.5–0.6) and the correlations are found for all radio frequencies, the optical–radio delays found around 2.1–2.4 yr do not represent strong evidence for a real physical correlation, because the time-scales suggested are too long. On the other hand, shorter delays around 33, 190 and 500 d are not significant, because they are found with low correlation coefficients. To investigate the radio–optical delays better, it is necessary to increase data sampling in future optical monitoring programmes.

3 RADIO FLUX VARIABILITY

The radio flux autocorrelation curves [discrete autocorrelation function (DACF) and Fisher z-transformed DACF (ZDACF)] of GC 0109+224 in various bands (Fig. 4) do not show very relevant features, except for broad and weak (ZDACF $\simeq 0.6$) peaks around the time-scale of 3.14–4.06 yr in the 14.5-GHz curve, and around 3.53–4.60 yr in the 37-GHz curve. From 37 to 14.5 GHz the autocorrelation profile resembles shot noise, with a single bump in the correlation curve of semi-amplitude $\simeq 2.7$ yr.

In Fig. 5 we plot the first-order structure functions (SFs) (e.g. Simonetti, Cordes & Heeschen 1985; Hughes, Aller & Aller 1992) of the radio light curves. The SF works in the time domain instead of frequencies f. It measures the mean difference in the data train as a function of the separation time Δt in the sampling. In log–log plots the SF of an ideal time series plus measurement noise increases and shows an intermediate steep curve [$\mathrm{SF}(\Delta t) \propto (\Delta t)^{\beta}$]. The slope β depends on the nature of the intrinsic variability, and give the Fourier power-law index of the spectrum [say $P(f) \propto 1/f^{\beta+1}$, where f is the frequency]. The values of β for GC 0109+224 (Fig. 5) go from 0.39 ± 0.16 to 0.65 ± 0.08, meaning an intermediate variability mode, between pure flickering (pink noise, $\beta = 0$) and shot noise (red/brown noise, $\beta = 1$). Deep and steep drops in the SF plots

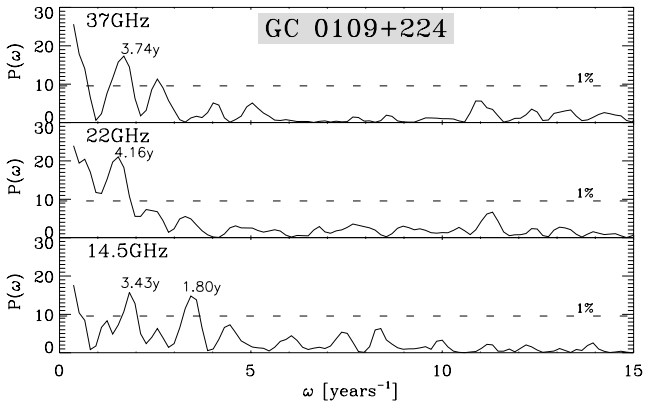

Figure 6. Periodogram plots of the 37, 22 and 14.5 GHz flux curves. Dotted lines shows the 1 per cent false alarm significance level, under the hypothesis of fluctuations dominated by Poisson statistics. The time-scales corresponding to the peaks above this level are 1.80, 3.43, 3.74 and 4.16 yr.

mean a small variance, and then a possible signature of characteristic time-scales: it is apparent at about 3.4–3.8 yr and 7.4–7.6 yr. Other characteristic time-scales are given by the turnover lag where the SF profile begins to flatten, and in the plots of Fig. 5 these are located around 1.1–1.8 yr, even if in our data the flattening is recognizable only with difficulties.

In Fig. 6 are reported the Lomb–Scargle periodograms (Scargle 1982; Horne & Baliunas 1986) of the radio curves, which present some features of interest. This technique [calculated with a fast algorithm (Press & Rybicki 1989)], analogous to the Fourier analysis for unevenly sampled data sets, is useful to detect possible periodicity and typical time-scales. The components above the 1 per cent false alarm threshold, annotated in Fig. 6 (from 1.8 to 4.16 yr), are not very significant, and not easily visually identifiable in the flux light curves.

The length of the data record required to demonstrate a real recurrent time-scale depends on signal-to-noise ratio, systematic errors, regularity in sampling, nature of the measurements and the nature of the underlying variation. Even if the strength of the autocorrelations found is not high, from the beginning of the 1990s our radio sampling is sufficient at all five bands observed to consider these discovered hints of time-scales as a starting point in the search for recurrent times with future observations. As mentioned above, hints of a sort of periodicity (or at least of a typical time-scale) around 3–4 yr are found by applying all three methods. Future radio flux data, with increased sampling and extended observing period, and VLBI observations may or may not confirm this time-scale.

4 THE SPECTRAL ENERGY DISTRIBUTION

GC 0109+224 is a bright X-ray point source [$\nu F_\nu(1\ \mathrm{keV}) \gtrsim 10^{-13}$ erg cm^{-2} s^{-1}], known since the observation of the *HEAO-1* A2 experiment (Della Ceca et al. 1990) in 1978 January. The spectral energy distribution (SED) assembled with the available historical multiwavelength data is shown in Fig. 7 (references for data in figure caption), and is compatible with a smooth continuum given by a pure synchrotron component, like the classical BL Lac objects. In Table 1 we summarize properties and available multiwavelength fluxes of GC 0109+224. The SED data profile in Fig. 7 points out a synchrotron peak in the frequency range around the near-infrared, optical (and possibly near-ultraviolet) range. This strengthens the assumption that GC 0109+224 is an LBL or intermediate blazar, as suggested for example in Laurent-Muehleisen et al. (1999), Dennett-Thorpe & Marchã (2000) and Bondi et al. (2001).

Unfortunately, apart from one rather low EGRET upper limit, no data are available to check the presence of the inverse Compton (IC) emission bump (the few old X-ray observations seem to have a synchrotron origin). The 1-keV flux measured by the *ROSAT* PSPC instrument in 1990 August is $F_\mathrm{X} = 0.26 \pm 0.08$ μJy, with $\alpha_\mathrm{X} = 1.96 \pm 0.25$ (Table 1 and Fig. 7). This suggests a decreasing soft X-ray trend in the νF_ν representation. The 1-keV flux measured by the *EXOSAT* CMA instrument in 1984 August is approximately the same ($F_\mathrm{X} = 0.21$ μJy), while the 2-keV flux measured by the *Einstein* Observatory (*HEAO-2*) IPC and MPC instruments in 1979 July is $F_\mathrm{X} = 0.15$ μJy. These detections seem to prove that the highest-energy synchrotron tail is emitted in the soft X-ray band (as is commonly found in intermediate blazars).

IRAS measured a flux density of 188 mJy at 60 μm and upper limits at its other bands (Impey & Neugebauer 1988). As cited above, GC 0109+224 seems to be characterized by a very strong (2–3 Jy) millimetre flux (apart from calibration uncertainties). On 2000 March 29, the IRAM Mambo bolometer measured a flux of 3.13 and 3.31 Jy at 1.2 mm (250 GHz), and the few other available measurements are all above 1 Jy (Bertoldi, private communication). On 2000 April 26, Metsähovi detected a flux above 2 Jy at 87 GHz (Fig. 2 and Table 1). No simultaneous optical data were available during this period in which the source is not visible at night, but 2000 February observations suggest a relevant high emission state [$F_\nu(0.44\ \mu\mathrm{m}) \simeq 16$ mJy]. According to Valtaoja & Teräsranta (1996), Jorstad et al. (2001), γ-ray flares are considered connected to the rising or high state of the blazar millimetre emission. GC 0109+224 seems to be on a rising phase during 1992 September as shown by the radio flux curves, but it was not detected in γ-rays by EGRET. This could contradict the cited hypothesis, or the γ-rays were of short duration, or again probably the sensitivity was inadequate. The integral flux density upper limit (UL) above 100 MeV is rather low: the limit given in the first EGRET catalogue (phase 1, 1991 April–1992 November) is $F_\gamma < 6 \times 10^{-8}$ photon cm^{-2} s^{-1}, approximately equivalent to 1 nJy. The low optical brightness and the small radio fluxes (sub-Jansky), reported in Table 2, in correspondence with the EGRET viewing periods, point out a low or, in any case, non-flaring state. For details on the EGRET viewing periods pertaining to GC 0109+224, and corresponding available optical and radio fluxes, see Table 2.

We tentatively fitted the few available data with a pure one-zone homogeneous leptonic SSC model, in two representative (low and high) states of the source (continuous lines in Fig. 7 for the 1990 August–October quiescent state, and the 2000 December flaring state). The multiwavelength SED data are grouped in epochs in Fig. 7 (but we remark that this is only a rough incongruent and temporally broad regrouping of the data). The applied model assumes a blob of dimension R embedded in a tangled isotropic magnetic field of mean intensity B, subjected to a continuous injection of shocked relativistic electrons with a break power-law energy distribution, exponentially damped: $Q_\mathrm{inj}(\gamma) = Q_0 \gamma^{-p} \exp[-\gamma/(k\gamma_\mathrm{max})]$ cm^{-3} s^{-1}, between the energies (Lorentz factors) γ_min and γ_max. This emitting region moves in a relativistic jet, approximately aligned with our line of sight and fed by an accreting supermassive black hole. The mechanism is described using a one-dimensional and time-dependent kinetic equation for the electron particle distribution, and the ensemble synchrotron spectrum is convolved with the calculated distribution. The IC spectrum results from the interaction of the distribution with the synchrotron photon field. The produced spectra

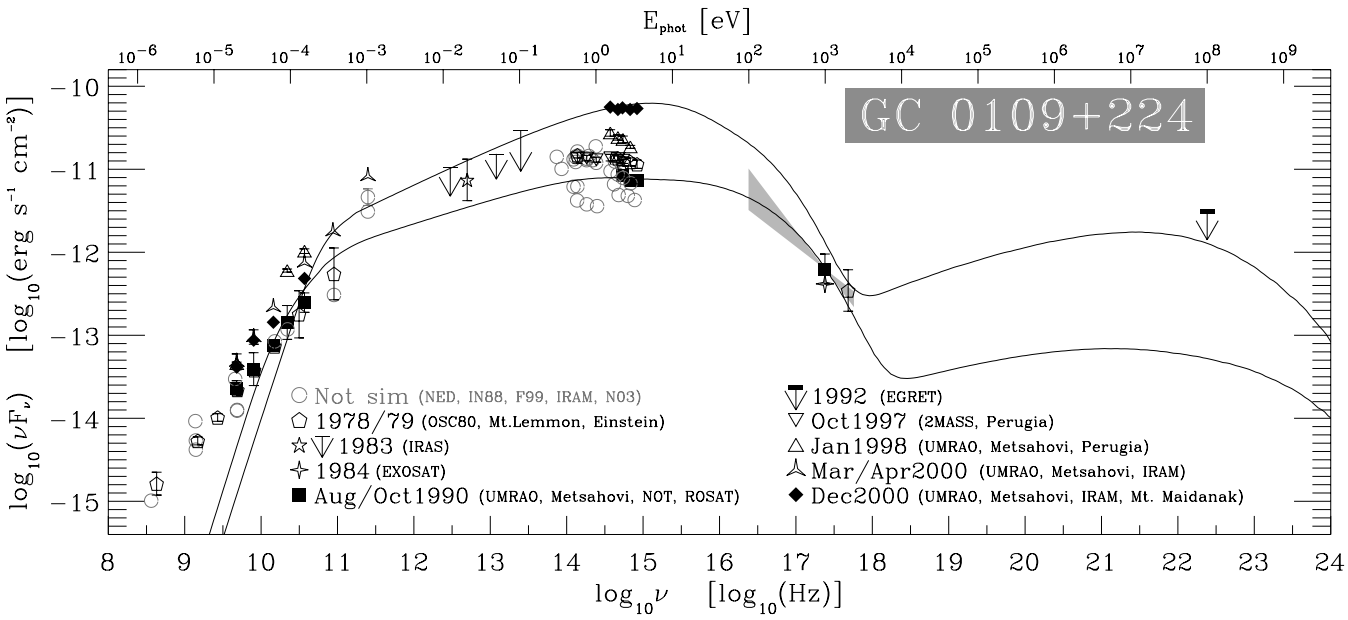

Figure 7. The SED of GC 0109+224 assembled with the available multiwavelength data (open and filled symbols), upper limits (arrows) and *ROSAT* slope (bow-tie), at different epochs. Two SSC model fit attempts (black lines) are used, for a low emission state and a high state. The SED is consistent with a pure smooth synchrotron continuum, peaking in the near-IR, optical, near-UV range. EGRET upper limit above 100 MeV is rather low. There is no evidence of γ-ray emission bump, and the few X-ray detections suggest a downward trend. Data are grouped for non-simultaneous epochs with the same symbol. Instruments or references are indicate in parentheses. Data from: this work (UMRAO, Metsähovi and Perugia observatories); NED data base (Owen et al. 1980 OSC80); Mt Lemmon (Puschell & Stein 1980), and from (Fan 1999, F99; Nesci et al. 2003, N03); *Einstein* IPC (Owen et al. 1981; Ledden & Odell 1985); *IRAS* (Impey & Neugebauer 1988, IN88); *EXOSAT* CMA (Maraschi & Maccagni 1988; Giommi et al. 1990; Reynolds et al. 1999); NOT (Valtaoja et al. 1993); *ROSAT* PSPC (Neumann et al. 1994; Brinkmann et al. 1995; Kock et al. 1996; Reich et al. 2000); EGRET (Fichtel et al. 1994; Hartman et al. 1999); 2MASS (Skrutskie et al. 1997); IRAM Mambo (00Mar, 01Jan and 02Jan, Bertoldi, private communication); and Mt Maidanak (Ciprini et al. 2003a). The two lines referring to the SSC fit attempts for the flaring state of 2000 December and the low state around the *ROSAT* detection in 1990 are performed with the following parameters. 1990 August/October low state: $\gamma_{\rm min} = 60$, $\gamma_{\rm max} = 1.7 \times 10^6$, $\gamma_{\rm break} = 5 \times 10^3$, $p_1 = 2.4$, $p_2 = 2.5$, $k = 0.015$, $B = 0.45$G, $R = 9.5 \times 10^{16}$cm, $\mathcal{D} = 13$. 2000 December high state: $\gamma_{\rm min} = 20$, $\gamma_{\rm max} = 5 \times 10^5$, $\gamma_{\rm break} = 7 \times 10^3$, $p_1 = 2.1$, $p_2 = 2.2$, $k = 0.015$, $B = 1.6$G, $R = 8.5 \times 10^{16}$cm, $\mathcal{D} = 15$. Redshift $z = 0.4$ is assumed (Falomo 1996).

were transformed to the frame of the observer (placed at an angle θ respect to the jet direction), using the relativistic Doppler beaming bulk factor $\mathcal{D} = [(1+z)\Gamma(1-\beta\cos\theta)]^{-1}$. The model is described for example in (Ciprini & Tosti 2003; Ciprini 2003). The values of the parameters adopted for the two SED parametrizations of GC 0109+224 are reported in the figure caption. The steep injection ($p > 2$) and the exponential damping create a few high-energy electrons (important for the IC emission). Moreover the relatively high value of B used (0.45–1.6 G) means a stronger magnetic field energy density $U_B = B^2/(8\pi)$ and a smaller radiation to magnetic energy ratio $U_{\rm rad}/U_B = L_{\rm IC}/L_{\rm syn}$, reducing the self-Compton flux. Indeed in our modelling (Fig. 7) the IC component appears depressed. The few multiwavelength data available do not contain any hint of a high-energy spectral component. The values used for the physical parameters partially take into account the radio flux data in the SED. For example, lower values of $\gamma_{\rm min}$ could fit better the lower-frequency radio data, but the IC emission is further depressed. The synchrotron spectral shape indicated by the available data appears also to be suitable for a fit with logarithmic parabolic functions (see e.g. Sambruna, Maraschi & Urry 1996; Giommi et al. 2002). Probably, as stated for the flux curves, the dynamics and the regions involved in the high-energy emission are different from the radio ones. Anyway the usual neglect of the radio data points in blazar SED modelling is almost never justified.

SED data and modelling (Fig. 7) allude to a synchrotron peak ranging between the near-IR, for the quiescent states, and the optical (perhaps also near-UV) bands, for the flaring states. This is consistent with the view of GC 0109+224 as a blazar at the border of the LBL and intermediate subclasses. As a classical BL Lac, the SED is represented well with our pure leptonic SSC model. Therefore, with simple scaling considerations, the IC emission can be seen as the synchrotron component upshifted by $\gamma^2_{\rm max}$ (with $\gamma_{\rm max} \simeq 10^5$ in this case). The peak in the optical, in SSC descriptions, can predict a possible IC peak in GeV γ-ray energies through the following similarity relation: $(\nu_{\rm GeV}F_{\rm GeV})/L_{\rm IC} \simeq (\nu_{\rm opt}F_{\rm opt})/L_{\rm syn}$ [as the synchrotron X-ray tail is related to the TeV γ-ray tail in HBLs (Stecker, de Jager & Salamon 1996)]. $L_{\rm syn}$ and magnetic field intensity might be high for this object, reducing the IC dominance. However, the strong millimetre flux, the peak of the SED in near-IR–optical bands and the brightness in X-ray frequencies might suggest the possibility of γ-ray emission. This emission may be detectable by the next generation of γ-ray satellites with improved sensitivity (e.g. *AGILE* and *GLAST*). Moreover, we note the possible correlation of GC 0109+224 with one of the highest-energy cosmic-ray events ever detected, $E = (1.7$–$2.6) \times 10^{20}$ eV, on 1993 December 3 (Farrar & Biermann 1998). In evading the Greisen–Zatsepin–Kuzmin (GZK) cut-off scenario, the primaries produced by particle acceleration in a blazar should travel extragalactic distances undeflected, pointing directly to its source, and under this assumption the probability of a coincidental alignment of that event with GC 0109+224 was only 0.5 per cent (Farrar & Biermann 1998).

Table 1. Some properties and fluxes of GC 0109+224. (1) Optical counterpart *Hipparcos* coordinates (Zacharias et al. 1999). (2) Redshift lower limit (Falomo 1996). (3) 82-cm flux density (Douglas et al. 1996). (4) 20-cm flux density (Owen, Spanger & Cotton 1980). (5) Mean flux densities from this work. (6) 87-GHz flux from Metsähovi. (7) 1.2-mm Mambo IRAM detection (Bertoldi, private communication). (8) *IRAS* far-IR flux at 60 μm (Impey & Neugebauer 1988). (9) Mid-IR flux in *L* band (Odell et al. 1978). (10) Mean optical flux in Cousins *R* band (Ciprini et al. 2003a). (11) Mean optical flux in Johnson *B* band from historical light curve (Ciprini et al. 2003a). (12) Optical (*B* band) minimum and maximum degrees of linear polarization (Takalo 1991; Valtaoja et al. 1993). (13) X-ray flux at 2 keV by *Einstein Observatory* (*HEAO-2*) IPC and MPC instruments (Owen, Helfand & Spangler 1981; Ledden & Odell 1985; Maraschi et al. 1986). (14) X-ray flux at 1 keV by CMA instrument on *EXOSAT* (Maraschi & Maccagni 1988; Giommi et al. 1990; Reynolds et al. 1999). (15) X-ray flux at 1 keV by PSPC instrument of *ROSAT* (Neumann et al. 1994; Brinkmann et al. 1995; Reich et al. 2000) and spectral index (Kock et al. 1996; Laurent-Muehleisen et al. 1999). (16) Flux limit above 100 MeV by EGRET (see Table 2) (Fichtel et al. 1994).

Quantity	Value	Epoch	Ref.
$RA(J2000.0)_{opt}$	$01^h12^m05\overset{s}{.}8238$	...	(1)
$Dec.(J2000.0)_{opt}$	$+22^\circ44'38\overset{''}{.}798$	...	(1)
z	>0.4	...	(2)
F_ν(0.365 GHz)	0.279 ± 0.021 Jy	...	(3)
F_ν(1.484 GHz)	0.36 ± 0.2 Jy	1978 Jan	(4)
$\langle F_\nu(4.8\ \mathrm{GHz})\rangle$	0.56 Jy	80Feb–01Dec	(5)
$\langle F_\nu(8\ \mathrm{GHz})\rangle$	0.67 Jy	78May–01Dec	(5)
$\langle F_\nu(14.5\ \mathrm{GHz})\rangle$	0.66 Jy	79Sep–01Dec	(5)
$\langle F_\nu(22\ \mathrm{GHz})\rangle$	1.07 Jy	85Jan–01Dec	(5)
$\langle F_\nu(37\ \mathrm{GHz})\rangle$	1.05 Jy	84Jul–01Aug	(5)
F_ν(87 GHz)	2.06 ± 0.09 Jy	2000 Apr 26	(6)
F_ν(250 GHz)	3.31 ± 0.06 Jy	2000 Mar 29	(7)
F_ν(60 μm)	188 mJy	1983	(8)
F_ν(3.5 μm)	11.8 mJy	1977 Jan	(9)
$\langle F_\nu(0.64\ \mu\mathrm{m})\rangle$	3.8 ± 0.2	94Nov–02Feb	(10)
$\langle F_\nu(0.44\ \mu\mathrm{m})\rangle$	2.4 ± 0.3	76Nov–02Feb	(11)
$P(B)_{min/max}$	0.7/29.69 per cent	...	(12)
F_ν(2 keV)	0.15 μJy	1979 Jul	(13)
F_ν(1 keV)	0.21 μJy	1984 Aug	(14)
F_ν(1 keV)	0.26 ± 0.08 μJy	1990 Aug	(15)
α_X	1.96 ± 0.25	1990 Aug	(15)
F_ν(>100 MeV)	<0.01 nJy	1992	(16)

5 SUMMARY AND CONCLUSIONS

In this work we have reported and analysed the largest amount of radio and optical data ever published on the BL Lac object GC 0109+224, collected over more than 20 years, and we have also reconstructed the most complete multiwavelength SED available. Some results are found, but also open questions are raised. GC 0109+224 is an example of a blazar which can produce strong outburst at high radio frequencies (2–3 Jy at $\nu \gtrsim 20$ GHz), but can remain relatively quiet ($\simeq 0.3$ Jy GB6 survey) for long periods. The flux density variability is characterized by intermittent behaviour, with an irregular alternation of relatively large-amplitude flares and flickering phases, in both radio and optical regimes. The source varies over all time-scales sampled (days, months, years). Optical flares are clearly much faster with respect to the radio–millimetre bands, and some particularly large optical outbursts do not have obvious counterparts at millimetre and radio wavelengths. This could suggest additional or different emitting components responsible for the radio and the optical emissions, and/or more rapid cooling of the synchrotron particles at higher frequencies. Moreover, radio flares, due to the longer duty cycles, can blend, inhibiting the identification of the radio counterparts of optical flares.

The radio light curves appear well correlated at the different frequencies, around the zero lag. The radio–optical cross-correlation peaks, found in all the bands around the lag of 2.1–2.4 yr, are extended and have low values (ZDCCF < 0.62). The complexity, spread and low values of the correlation peaks, the impossibility of visually recognizing the lags in the light curves, the very different duty cycles and especially such long delays suggest that there is no real correlation, and no physical meaning in the two-year lag. Other shorter delays around 33, 190 and 500 d are not significant because they are found with very small correlation coefficients. Fig. 3 shows also that the signal is weak at zero time lag (between optical and 37–22 GHz curves). This means that strong events in the optical bands do not have a simultaneous recognizable counterpart in the radio bands. Maybe additional processes and/or different regions are responsible for the emission at different frequencies (optical photons could be generated into jet components of different size and dynamics, in correspondence to the radio emission). A certain level of confusion is undoubtedly created by induced causes (i.e. the large empty gaps in the optical light curve data).

Table 2. EGRET viewing periods (VP) and flux upper limits (UL) of GC 0109+224. Related quasi-simultaneous radio and optical fluxes from this work are also reported when available. References: (a) EGRET integral flux density upper limit above 100 MeV (first EGRET catalogue, phase 1) for three VP 0260, 0280, 0370, (Fichtel et al. 1994); (b) the only simultaneous optical data available (Valtaoja et al. 1993) point out a low brightness and polarization degree 5.20 ± 0.61; (c) UL given by the summed exposures of phase 1 pointings, and the other EGRET VP of the GC 0109+224 region on phase 3 and cycle 4 (1994–95) (Hartman et al. 1999). Any new pointing of the region was done during the EGRET phase 2 (1992Nov–1993Sep, Thompson et al. 1995). During EGRET cycle 8, at least one more pointing was available (2000 Apr 18–25) but our source was on the edge of the field of view. Throughout in all the EGRET VP the source had a relatively low (sub-Jy) radio emission.

EGRET VP	Start–end date	F_γ(>100 MeV) (photon cm^{-2} s^{-1})	Ref.	Optical obs. epoch	F_{opt} (mJy)	Ref.	Radio obs. epoch	F_{rad} (Jy)
0260...	1992 Apr 23–28			...	...		1992 Apr 26	$F_{14.5} = 0.48 \pm 0.03$
0280...	1992 May 07–14	$<6.0 \times 10^{-8}$	(a)	...	...		1992 Apr 29	$F_{37} = 0.58 \pm 0.13$
0370...	1992 Aug 20–27			1992 Aug 28	0.94 ± 0.03	(b)	1992 May 06	$F_{14.5} = 0.33 \pm 0.01$
...	...	...		...	...		1992 Sep 01	$F_{22} = 0.94 \pm 0.03$
3170...	1994 Feb 17–Mar 01			...	...		1994 Mar 15	$F_{22} = 0.78 \pm 0.11$
4250...	1995 Jul 25–Aug 08	$<5.6 \times 10^{-8}$	(c)	...	...		1995 Jul 20	$F_{22} = 0.75 \pm 0.04$
...	...	...		...	...		1995 Aug 04	$F_{22} = 0.83 \pm 0.05$
...	...	...		...	...		1995 Aug 06	$F_{37} = 0.91 \pm 0.06$

Only continuous monitoring over longer periods, with reduced gaps, will clarify the existence of physical radio–optical delays in this source.

The DCF and SF shapes reflect the underlying nature of the process that created the radio variability. Both methods demonstrate, for GC 0109+224, a fluctuation mode between flickering and shot noise [i.e. $P(f) \propto 1/f^{\alpha}$], with $1.39 < \alpha < 1.65$. A similar behaviour was also found for the optical emission (Ciprini et al. 2003a,b) of this source. This power spectrum is characteristic of a random walk. In the case of the best-sampled 22-GHz light curve, the value $\alpha = 1.65$ found is in strict agreement with the 5/3 value for fully developed turbulence in the scalar theory of Kolmogorov. Such variability could be related to fluctuations of the magnetic field, or of the bulk motion velocity of the emitting regions inside the jet.

There is no evidence from our data for long-term periodic variations with a fixed period, but typical time-scales in the ranges of ∼3.2–4.5 yr are implied, with all the applied methods (DCF, SF, periodogram). The more rapid flickering synchrotron peaks seem superimposed on to long-term trends in the radio. This could also be the result of flares blending with long cooling times, as mentioned above.

The increased activity and mean flux level, well observed in all the radio–optical bands, suggest that the same emission mechanism is responsible for radiation in both spectral regimes, i.e. the synchrotron radiation from shocked plasma into the jet, as seen also in the SED. Synchrotron emission in GC 0109+224 is probably dominant and powerful ($L_{\rm syn}/L_{\rm IC} > 1$), as suggested by the high degree of polarization, and by the absence of emission lines (z is still undetermined). The relatively high degree of linear polarization observed could mean a weaker connection with the usual depolarization effects, which is a common affliction of blazar jets (like the influence of a luminous host galaxy). The overall SED of GC 0109+224 shows a smooth synchrotron continuum peaked in the near-IR–optical range (as shown by intermediate blazars). Also our homogeneous SSC modelling suggests a relatively high magnetic field and synchrotron luminosity, diminishing the self-Compton radiation, even though the multiwavelength data reported are insufficient to fully constrain the model. In particular, GC 0109+224 suffers from substantial lack of data in millimetre, submillimetre and infrared bands, to check the importance of a possible thermal emission component (and also the possibility of external Compton contributions).

Despite the common deficiency of infrared data, and difficulties for far- and mid-IR blazar monitoring, we suggest at least millimetre observations, due to the intense radiation that GC 0109+224 seems to produce at these frequencies. X-ray observations of this blazar are also strongly encouraged, to check for the presence of the high-energy component in the spectrum. The high-energy predictions for an intermediate blazar suffer uncertainties that become relevant in high-energy tails, even when only using leptonic models (Böttcher, Mukherjee & Reimer 2002). Moreover, the X-ray data are insufficient to permit any prediction about TeV γ-rays from this object (due to the suggested $z > 0.4$, TeV emission might be interesting for studies on the extragalactic background light by absorption cut-offs). However, millimetre brightness, and synchrotron emission peaked at optical frequencies, could imply a GeV γ-ray radiation detectable by the next generation of γ-ray space telescopes. An increased observing effort for this source, especially at X-ray bands and beyond [for example, GC 0109+224 is just scheduled to be observed by *Integral* (Pian 2002)], together with a better monitoring in radio–millimetre–optical bands, will clarify some of the questions that have arisen in our data and analysis. In this view our data and work will be a useful data base.

ACKNOWLEDGMENTS

We wish to thank Kyle Augustson for useful comments. The Metsähovi Radio Observatory is an institute of the Helsinki University of Technology, partially financed by the Academy of Finland. The UMRAO is supported by the US National Science Foundation, and by funds from the University of Michigan. The optical monitoring programme of the Perugia University Observatory was partly supported by the Italian MIUR under grant Cofin2002. The European Institutes belonging also to the ENIGMA collaboration acknowledge EC funding under contract HPRN-CT-2002-00321. This research has made use also of the Simbad data base (CDS, Strasbourg), the NASA/IPAC Extragalactic Database NED (JPL, CalTech and NASA), the HEASARC data base (LHEA, NASA/GSFC and SAO), and NASA's ADS digital library.

REFERENCES

Alexander T., 1997, in Maoz D., Sternberg A., Leibowitz E. M., eds, Astronomical Time Series. Kluwer, Dordrecht, p. 163
Aller H. D., Aller M. F., Hughes P. A., 1996, in Miller H. R., Webb J. R., Noble J. C., eds, ASP Conf. Ser. Vol. 110, Blazar Continuum Variability. Astron. Soc. Pac., San Francisco, p. 208
Aller M. F., Aller H. D., Hughes P. A., Latimer G. E., 1999, ApJ, 512, 601
Bondi M., Marchã, M. J. M., Dallacasa D., Stanghellini C., 2001, MNRAS, 325, 1109
Böttcher M., Mukherjee R., Reimer A., 2002, ApJ, 581, 143
Brinkmann W., Siebert J., Reich W., Fuerst E., Reich P., Voges W., Truemper J., Wielebinski R., 1995, A&AS, 109, 147
Ciprini S., 2003, New Astron. Rev., 47, 709
Ciprini S., Tosti G., 2003, in Takalo L. O., Valtaoja E., eds, ASP Conf. Ser. Vol. 299, High Energy Blazar Astronomy. Astron. Soc. Pac., San Francisco, p. 269
Ciprini S., Tosti G., Raiteri C. M., Villata M., Ibrahimov M. A., Nucciarelli G., 2003a, A&A, 400, 487
Ciprini S., Fiorucci M., Tosti G., Marchili N., 2003b, in Takalo L. O., Valtaoja E., eds, ASP Conf. Ser. Vol. 299, High Energy Blazar Astronomy. Astron. Soc. Pac., San Francisco, p. 265
Della Ceca R., Palumbo G. G. C., Persic M., Boldt E. A., Marshall E. E., de Zotti G., 1990, ApJS, 72, 471
Dennett-Thorpe J., Marchã M. J., 2000, A&A, 361, 480
Douglas J. N., Bash F. N., Bozyan F. A., Torrence G. W., Wolfe C., 1996, AJ, 111, 1945
Edelson R. A., Krolik J. H., 1988, ApJ, 333, 646
Falomo R., 1996, MNRAS, 283, 241
Fan J. H., 1999 (astro-ph/9910269)
Farrar G. R., Biermann P. L., 1998, Phys. Rev. Lett., 81, 3579
Fey A. L., Charlot P., 2000, ApJS, 128, 17
Fichtel C. E., Bertsch D. L., Chiang J. et al., 1994, ApJS, 94, 551
Gaskell C. M., Peterson B. M., 1987, ApJS, 65, 1
Giommi P., Barr P., Garilli B., Maccagni D., Pollock A. M. T., 1990, ApJ, 356, 432
Giommi P. et al., 2002, in Giommi P., Massaro E., Palumbo G., eds, ASI Spec. Publ., Blazar Astrophysics with BeppoSAX and Other Observatories. ESA-ESRIN, Rome, p. 63
Hanski M. T̃., Takalo L. Õ., Valtaoja E., 2002, A&A, 394, 17
Hartman R. C., Bertsch D. L., Bloom S. D. et al., 1999, ApJS, 123, 79
Horne J. H., Baliunas S. L., 1986, ApJ, 302, 757
Hufnagel B. R., Bregman J. N., 1992, ApJ, 386, 473
Hughes P. A., Aller H. D., Aller M. F., 1992, ApJ, 396, 469
Impey C. D., Neugebauer G., 1988, AJ, 95, 307
Jorstad S. G., Marscher A. P., Mattox J. R., Aller M. F., Aller H. D., Wehrle A. E., Bloom S. D., 2001, ApJ, 556, 738
Kock A., Meisenheimer K., Brinkmann W., Neumann M., Siebert J., 1996, A&A, 307, 745
Laurent-Muehleisen S. A., Kollgaard R. I., Feigelson E. D., Brinkmann W., Siebert J., 1999, ApJ, 525, 127

Ledden J. E., Odell S. L., 1985, ApJ, 298, 630
Maraschi L., Maccagni D., 1988, Mem. Soc. Astron. Ital., 59, 277
Maraschi L., Ghisellini G., Tanzi E. G., Treves A., 1986, ApJ, 310, 325
Marchã M. J. M., Browne I. W. A., Impey C. D., Smith P. S., 1996, MNRAS, 281, 425
Mead A. R. G., Ballard K. R., Brand P. W. J. L., Hough J. H., Brindle C., Bailey J. A., 1990, A&AS, 83, 183
Nesci R., Sclavi S., Maesano M., Massaro E., Dolci M., D'Alessio F., 2003, Mem. Soc. Astron. Ital., 74, 169
Neumann M., Reich W., Fürst E., Brinkmann W., Reich P., Siebert J., Wielebinski R., Truenper J., 1994, A&AS, 106, 303
Odell S. L., Puschell J. J., Stein W. A., Owen F., Porcas R. W., Mufson S., Moffett T. J., Ulrich M.-H., 1978, ApJ, 224, 22
Owen F. N., Mufson S. L., 1977, AJ, 82, 776
Owen F. N., Spanger S. R., Cotton W. D., 1980, AJ, 85, 351
Owen F. N., Helfand D. J., Spangler S. R., 1981, ApJ, 250, 550
Padovani P., Giommi P., 1995, ApJ, 444, 567
Pauliny-Toth I. I. K., Kellermann K. I., Davis M. M., Fomalont E. B., Shaffer D. B., 1972, AJ, 77, 265
Pian E., 2002, Blazar TOO, Integral Ann. of Opp.(AO-1)
Press W. H., Rybicki G. B., 1989, ApJ, 338, 277
Puschell J. J., Stein W. A., 1980, ApJ, 237, 331
Reich W., Fuerst E., Reich P., Kothes R., Brinkmann W., Siebert J., 2000, A&A, 363, 141
Reynolds A. P., Parmar A. N., Hakala P. J., Pollock A. M. T., Williams O. R., Peacock A., Taylor B. G., 1999, A&AS, 134, 287
Sambruna R. M., Maraschi L., Urry C. M., 1996, ApJ, 463, 444
Scargle J. D., 1982, ApJ, 263, 835
Simonetti J. H., Cordes J. M., Heeschen D. S., 1985, ApJ, 296, 46
Sitko M. L., Schmidt G. D., Stein W. A., 1985, ApJS, 59, 323
Skrutskie M. F. et al., 1997, in Garzon F., ed., The Impact of Large Scale Near-IR Sky Surveys. Kluwer, Dordrecht, p. 25
Stecker F. W., de Jager O. C., Salamon M. H., 1996, ApJ, 473, L75
Tagliaferri G., Ghisellini G., Giommi P. et al., 2000, A&A, 354, 431
Takalo L. O., 1991, A&AS, 90, 161
Teräsranta H., 2002, in Giommi P., Massaro E., Palumbo G., eds, ASI Spec. Publ., Blazar Astrophysics BeppoSAX and Other Observatories. ESA-ESRIN, Rome, p. 215
Teräsranta H., Tornikoski M., Mujunen A. et al. 1998, A&AS, 132, 305
Thompson D. J., Bertsch D. L., Dingus B. L. et al., 1995, ApJS, 101, 259
Tosti G., Massaro E., Nesci R., Ciprini S. et al., 2002, A&A, 395, 11
Valtaoja E., Teräsranta H., 1996, A&AS, 120, 491
Valtaoja L., Sillanpää A., Valtaoja E., Shakhovskoi N. M., Efimov I. S., 1991, AJ, 101, 78
Valtaoja L., Karttunen H., Efimov Y. S., Shakhovskoy N. M., 1993, A&A, 278, 371
Wilkinson P. N., Browne I. W. A., Patnaik A. R., Wrobel J. M., Sorathia B., 1998, MNRAS, 300, 790
Wright S. C., McHardy I. M., Abraham R. G., Crawford C. S., 1998, MNRAS, 296, 961
Zacharias N., Zacharias M. I., Hall D. M., Johnston K. J., de Vegt C., Winter L., 1999, AJ, 118, 2511

This paper has been typeset from a TEX/LATEX file prepared by the author.